Hunting for WIMPs with the Cryogenic Dark Matter Search

S.R. GOLWALA[10], D.S. AKERIB[1], P.D. BARNES, Jr.[4], D.A. BAUER[11], A. BOLOZDYNYA[1], P. BRINK[9], B. CABRERA[9], D.O. CALDWELL[11], J.P. CASTLE[8], R.M. CLARKE[9], P. COLLING[9], M.B. CRISLER[2], A. DA SILVA[10], A.K. DAVIES[9], R. DIXON[2], S. EICHBLATT[2], K.D. IRWIN[5], R.J. GAITSKELL[10], E.E. HALLER[3], J. HELLMIG[10], M.E. HUBER[12], J. JOCHUM[10], F.P. LIPSCHULTZ[8], J. MARTINIS[5], S.W. NAM[9], H. NELSON[11] B. NEUHAUSER[8], T.A. PERERA[1], R.R. ROSS[3], T. SAAB[9], B. SADOULET[10], R.W. SCHNEE[1], P. SHESTOPLE[8], T. SHUTT[6], A. SMITH[3], A.H. SONNENSCHEIN[11], A.L. SPADAFORA[10], S. YELLIN[11], B.A. YOUNG[7]

(1) Department of Physics, Case Western Reserve University
Cleveland, OH 44106, USA

(2) Fermi National Accelerator Laboratory
Batavia, IL 60510, USA

(3) Lawrence Berkeley National Laboratory
Berkeley, CA 94720, USA

(4) Lawrence Livermore National Laboratory
Livermore, CA 94550, USA

(5) National Institute of Standards and Technology
Boulder, CO 80303, USA

(6) Department of Physics, Princeton University
Princeton, NJ 08544, USA

(7) Department of Physics, Santa Clara University
Santa Clara, CA 95053, USA

(8) Department of Physics and Astronomy, San Francisco State University
San Francisco, CA 94132, USA

(9) Department of Physics, Stanford University
Stanford, CA 94305, USA

(10) Center for Particle Astrophysics, University of California, Berkeley
Berkeley, CA 94720, USA

(11) Department of Physics, University of California, Santa Barbara
Santa Barbara, CA 93106, USA

(12) Department of Physics, University of Colorado
Denver, CO 80217, USA

Contact email: golwala@cfpa.berkeley.edu

Abstract. The Cryogenic Dark Matter Search (CDMS) is an experiment whose goal is to detect WIMPs via elastic-scattering interactions in detectors capable of nuclear-recoil discrimination. Recent advances in eliminating a low-energy-electron background are discussed. Data from the current run yield 1 nuclear-recoil candidate above 25 keV recoil energy in 1.7 kg-days of exposure.

1. Introduction

There is extensive evidence that a large fraction of the matter in the universe is nonluminous. In recent years, there has been a growing consensus that $\Omega_{\rm m}$ is greater than approximately 0.25, far greater than $\Omega_{\rm lum} \sim 0.003h^{-1}$ [1]. The discrepancy between $\Omega_{\rm m}$ and the range for $\Omega_{\rm b}$ given by the standard model of big bang nucleosynthesis, $0.006h^{-2} < \Omega_{\rm b} < 0.016h^{-2}$ (95% CL) [2], indicates a need for a large fraction of $\Omega_{\rm m}$ to be nonbaryonic. To match the factor by which density perturbations have grown between the time of radiation-baryon decoupling and today, it is necessary for much of the nonbaryonic dark matter to be "cold" - nonrelativistic at the time that gravitational collapse began.

Weakly Interacting Massive Particles, or WIMPs, are a candidate for nonbaryonic cold dark matter. WIMPs are a generic class of particles that are expected to be generated by physics at the electroweak scale. They would interact only via the weak interaction (and gravity) and would have mass of order 100 GeV. Such a particle δ would be produced in the early universe and would decouple while nonrelativistic, resulting in a relic abundance of $\Omega_\delta h^2 \sim 1$ [3]. Had the characteristic electroweak mass and weak interaction cross-section been different, the relic density would not be cosmologically interesting. This coincidence has long been taken as a hint at a connection between the need for dark matter and new particle physics beyond the electroweak scale. Minimal supersymmetry provides a natural WIMP candidate in the form of the lightest superpartner, which is stabilized by R-parity and would likely have no electromagnetic or strong interactions [4]. The parameter space of supersymmetric WIMPs has been discussed by A. Masiero in this volume.

The Cryogenic Dark Matter Search, or CDMS, is an experiment whose goal is to detect elastic scattering of WIMPs with nuclei in terrestrial targets. CDMS employs novel cryogenic detectors that, for each event, produce a phonon-mediated recoil-energy measurement and an ionization measurement. These detectors allow CDMS to have both a low recoil-energy threshold and extremely good discrimination against electromagnetic backgrounds. These two factors, combined with standard low-background-physics techniques, give CDMS an excellent sensitivity to WIMPs and an ability to probe minimal supersymmetry.

2. Detecting WIMPs

WIMPs are expected to have collapsed into a roughly isothermal spherical halo within which the visible portion of our galaxy resides. Thus, the WIMPs occupy a Maxwell-Boltzmann velocity distribution with velocity dispersion 270 km s^{-1}. The expected

spectrum of recoil energies due to WIMP-nucleus elastic-scattering events is discussed in [4] and [5]; it is exponential with characteristic recoil energy given by

$$Q_0 = \frac{2m_\delta^2 m_{\rm N}}{\left(m_\delta + m_{\rm N}\right)^2}\left(\frac{v_0}{c}\right)^2 \tag{1}$$

where m_δ is the WIMP mass, $m_{\rm N}$ is the target nucleus mass, and $v_0 \simeq 220$ km s^{-1} is the circular velocity of the Sun around the galactic center. For example, a 100 GeV WIMP incident on a germanium nucleus gives $Q_0 \simeq 13$ keV; Q_0 asymptotes to 41 keV for Ge as $m_\delta \to \infty$. The expected event rates depend on the exact model for the WIMP and are 1 kg^{-1} day^{-1} or lower. Thus, given the low energy deposition and event rate, a WIMP search experiment requires a threshold of a few keV and an extremely low rate of background – *i.e.*, non-WIMP – events.

3. Nuclear-Recoil Discrimination

One technique for rejecting background events is nuclear-recoil discrimination. WIMPs produce nuclear recoils, while nearly all irreducible background sources (primarily photons from natural radioactivity and radon daughters) produce electron recoils. This difference can be used to discriminate WIMP interactions from background events. In practice, there are a number of ways to perform discrimination via simultaneous measurement of two event parameters: recoil energy and scintillation (CRESST II), primary and secondary scintillation [6], and recoil energy and ionization. In the last case, the ionization yield (amount of ionization produced per unit recoil energy) for nuclear recoils is lower than that for electron recoils (by a factor of 3 is Ge). This fact is displayed graphically in Figure 1. Such a detector's ability to reject the irreducible photon background is excellent, greater than 99%.

4. CDMS Detectors

The CDMS detectors have three novel aspects that make CDMS potentially much more sensitive than other WIMP search experiments. First, CDMS uses a phonon-mediated recoil-energy measurement in detectors cooled to cryogenic temperatures, yielding superior energy resolution and hence lower threshold (see Figure 2). Second, phonon-mediated measurements give **total** recoil energy, irrespective of whether the interaction produces an electron or nuclear recoil, and hence provide an unquenched, direct measurement of the recoil energy deposited during a scattering event. Third and most importantly, CDMS combines a phonon-mediated measurement of the recoil energy with an ionization-yield measurement as described above, thereby providing rejection of the background of electron recoils while maintaining high acceptance for WIMP-produced nuclear recoils.

In order to perform the ionization meaurement, a drift field of a few V/cm is applied across 1 cm thick disk-shaped crystals using electrodes deposited on the top and bottom faces. The electrodes are segmented radially, yielding a central disk-shaped volume and an outer annular guard ring. The usefulness of such a design will be discussed later. A low-noise charge amplifier is connected to the biased electrode via a blocking capacitor. In contrast to standard ionization detectors, such as Ge gamma spectrometers, the CDMS detectors use a low drift field of a few V/cm, compared to hundreds of V/cm in gamma spectrometers. Use of a low field is possible in cryogenic

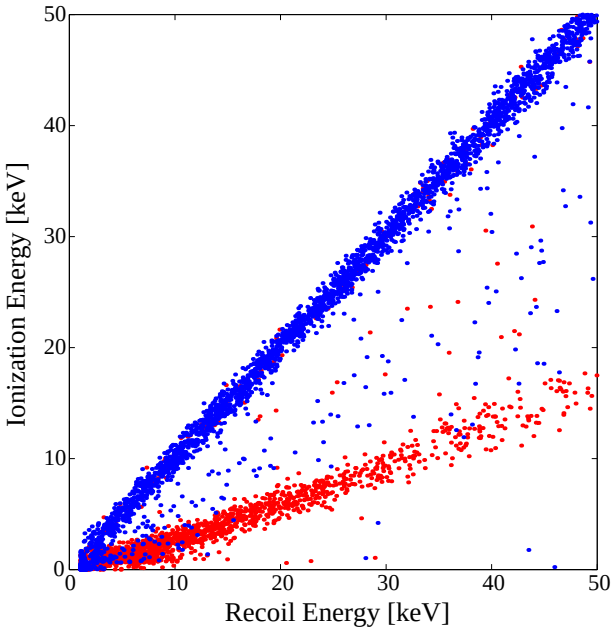

Figure 1. Demonstration of nuclear-recoil discrimination. Blue (dark) dots are events from exposure to ^{60}Co photon source, producing electron recoils. Red (light) dots are events from exposure to ^{252}Cf neutron source, producing nuclear recoils.

detectors because charge trapping sites that force the use of a large field at 77 K are frozen out at 20 mK. It is necessary to use a low field because heat is generated by drifting charges in proportion to the bias voltage (the Neganov-Luke effect); this extra heat is equal in size to the "intrinsic" heat signal at a bias of 3 V in Ge.

CDMS employs two different technologies for measuring recoil energy. CDMS first developed the Berkeley Large Ionization- and Phonon-mediated (BLIP) detector, in which the phonon measurement is done thermally. The measured quantity is the temperature change observed when a particle deposits energy in the detector. Two neutron transmutation doped (NTD) germanium thermistors are eutectically bonded to a 6 cm diameter, 1.2 cm thick, 165 g Ge crystal. At 20 mK, a 10 keV energy deposition in the crystal produces a 1 μK temperature change, yielding a resistance change of approximately 250 Ω (at ~ 2 MΩ operating resistance) and a voltage signal of about 2 μV. An aspect of the measurement shared with NTD Ge bolometers used in many CMB experiments is the use of a lock-in technique: the thermistors are biased with a 1 kHz sine wave current and the signal is demodulated after passing through the first stage amplifier. This moves the signal away from the low-frequency rise in the front end JFET noise. The BLIP energy resolution has been measured *in situ* using 10.4 keV ^{68}Ga X-rays arising from internal cosmogenic activation (see Figure 2).

More recently, CDMS has developed the Z-sensitive Ionization- and Phonon-mediated detector, or ZIP. ZIPs are fabricated from Si and Ge crystals, 7.6 cm in diameter, 1 cm thick, and weighing 100 g and 250 g, respectively. ZIPs employ athermal phonons to obtain greater information about the interaction than do the

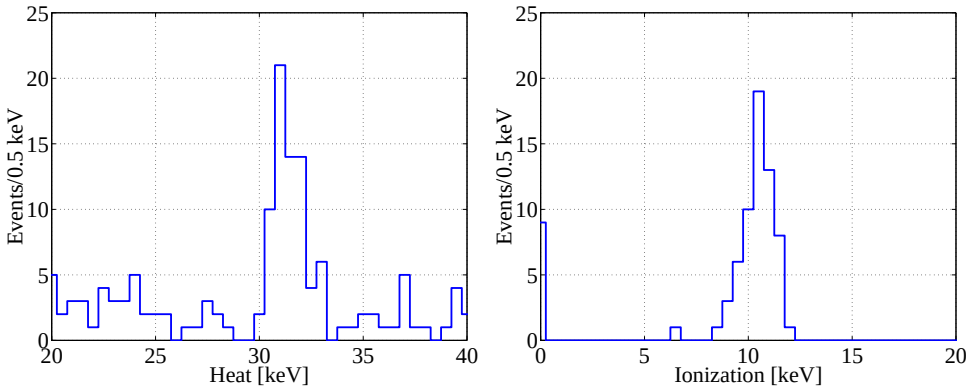

Figure 2. Detector resolution (BLIP detector). On the left is "heat" (phonon signal), on the right is ionization. The X-ray energy is 10.4 keV; due to the Neganov-Luke effect and the use of 6 V ionization bias, an additional 20.8 keV in heat is generated by ionization drift; hence the total heat is 31.2 keV.

BLIP thermal phonon-mediated detectors. Soon after a particle interaction occurs (within a few μs), high-energy (few Kelvin, and hence athermal) phonons propagate outward from the interaction point. These phonons travel on approximately straight line paths through the crystal. One surface of the detector is covered with large superconducting aluminum pads; the incoming high-energy phonons break Cooper pairs in the pads, producing quasiparticles (essentially electrons and holes) that may diffuse around the pads. Abutting the edges of the pads are thin strips of tungsten held in the middle of their superconducting transition by Joule heating and electrothermal feedback. Quasiparticles that reach the tungsten strips deposit their energy as they collapse back to the Fermi surface, raising the temperature, and hence resistance, of the tungsten. This reduces the current through the DC voltage-biased sensor. The input loop of a SQUID current amplifier is placed in series with the tungsten meanders, permitting the SQUID to sense and amplify the change in current. Electrothermal feedback stabilizes the detector response by reducing sensitivity to variations in tungsten T_c across a crystal and also to variations in the crystal temperature; it also reduces the pulse fall time to ~ 200 μs. The phonon sensor is segmented into four quadrants. The pulse rise times are sensitive to the arrival time of phonons at the quadrants, and hence relative arrival times can be used to locate an event in x and y. In addition, events occurring very near the surface (a few tens of μm) display faster rise times than bulk events, allowing one to veto surface events.

Thanks to the measurement of fast phonons, the ZIP detector displays a number of advantages over the BLIP detector: z position sensitivity permits vetoing of surface events; relative phonon pulse arrival times yield xy position information; phonon pulses with fast (tens of μs) rise times make it easier to find the associated ionization signal and, in the case that no such signal is found, to check for veto coincidences with only phonon information; 200 μs phonon pulse decay times reduce the amount of posttrigger sampling and hence improve live time; and the use of athermal phonons yields energy resolution independent of detector size (the BLIP detector's pulse height degrades with the crystal heat capacity and hence volume). For these reasons, BLIPs are currently being phased out in favor of ZIPs.

5. Low Background Facility, Shield, and Cryostat

The low rate of WIMP interactions necessitates operation at a site with low particle flux. CDMS operates its detectors in a tunnel 16 meters water equivalent underground at the Stanford Underground Facility (SUF) on the Stanford University campus. The flux of particles from the hadronic component of cosmic ray air showers is stopped by this overburden, and the muonic component is reduced by a factor of 5. This shallow site was chosen for the initial phase of CDMS due to its proximity to many of the participating institutions. CDMS has begun construction of infrastructure for operation at the Soudan mine in Minnesota, at 2070 mwe. At Soudan, the event rate will be dominated instead by photons from natural radioactivity. Operation of detectors there is expected to begin in mid-2000, pending funding approval.

Due to the low operating temperature (~ 20 mK) and need for extended running of CDMS detectors, a dilution refrigerator is required; however, commercial dilution refrigerators are constructed from stainless steel, brass, and aluminum, and contain solder – all materials with unacceptable radioactivity. To deal with this, CDMS constructed a radiopure right angle extension to an Oxford S-400 dilution refrigerator, the Icebox. This cryostat has operated for seven many-month runs at SUF since 1996. A duplicate cryostat is under construction for Soudan. The Icebox is made entirely from OFHC copper that was pre-screened for radioactive contamination. It consists of six concentric tubes extending out from the bottom of the dilution refrigerator that then connect to a set of six nested cans. The innermost can has a volume of approximately 30000 cm^3 and will hold 42 detectors. The Icebox is an engineering feat in and of itself due to the many thermal conduction, loading, and contraction issues in such a design; it has been described in great detail elsewhere [7].

The large muon flux ($\sim$ 40 m^{-2} s^{-1}) at the shallow Stanford site necessitates a highly efficient muon veto to tag muon-related events. Such a veto has been constructed using large plastic scintillator paddles; it completely encases the radiopure section of the cryostat. The veto has been measured to be $> 99.99\%$ efficient for muons passing through the detectors.

Inside the muon veto is a lead shield. Photons (and assorted other particles) are produced both by muon-induced reactions in the earth surrounding the tunnel and by natural radioactive decays of material in the tunnel walls and the dilution refrigerator. This shield reduces the photon flux incident on the detectors. Logistical and live time issues are raised by a high photon rate.

Neutron shielding is provided by 25 cm of polyethylene moderator between the lead shield and the cryostat. Muon interactions with nuclei can produce neutrons. The moderator stops neutrons produced by muons interacting in the lead shield, some of which may be delayed and hence would not be easily tagged as muon-coincident. In addition, the moderator attenuates neutrons produced in the tunnel walls; the associated muons usually have not passed through the veto. Monte Carlo simulations indicate that the neutron background at SUF will be no larger than 0.01 kg^{-1} keV^{-1} day^{-1}.

Finally, internal to the innermost can of the cryostat is an ancient lead shield, 1 cm thick. Ancient lead is low in ^{210}Pb, whose daughter ^{210}Bi decays by β-decay with a 1.16 MeV endpoint. These β's produce high energy photons by bremsstrahlung; hence the ancient lead shields the detectors from the intrinsic radioactivity of the outer lead shield. It also provides shielding against the intrinsic radioactivity of the copper cryostat.

The photon flux measured in the final setup is roughly 60 kg^{-1} keV^{-1} day^{-1} overall and 2 kg^{-1} keV^{-1} day^{-1} anticoincident with veto. This anticoincident rate is quite competitive with previous low-background experiments and reflects the care and study that went into construction of the shield and selection of materials for and assembly of the cryostat.

6. Prior Results and Electron Background

To frame the presentation of the current data, it is necessary to briefly discuss results from data taken during a previous run in spring 1998. Data were acquired with one Si ZIP and two Ge BLIP detectors, yielding 1.0 and 6.3 kg-days of exposure, respectively. Plots of ionization energy/recoil energy versus recoil energy for these detectors are shown in Figure 3. The vertical axis of these plots corresponds to dividing the vertical axis of Figure 1 by its horizontal axis and plotting against the horizontal axis. Electron recoils lie at 1 on the vertical axis; nuclear recoils lie at approximately 0.3.

A large number of events appear in the nuclear-recoil band for the BLIP detector. The distribution seems to tail upward to the electron-recoil band with increasing recoil energy. These events are believed to be due to low-energy electrons impinging on the surface of the detector. It has been known for some time that the ionization electrode technology used on the BLIP detectors suffers from a "dead layer" – a layer, of order 20 μm thick, below the electrode, for which ionization collection is artificially depressed. Hence, though electrons produce electron recoils, some of these dead layer events appear in the nuclear-recoil region of an ionization yield versus recoil energy plot. This effect has been seen with low-energy (< 20 keV) photons, which have a penetration depth of the same thickness as the dead layer. However, the continuation of this effect beyond 100 keV requires that the incident species have a very short penetration depth in this energy range. Electrons are an excellent candidate. In addition, there is a high rate of events with suppressed ionization collection below approximately 20 keV. These events fit a tritium β spectrum, again consistent with the electron hypothesis.

The phenomenology of the dead layer is straightforward: a particle interaction produces a cloud of electron-hole pairs that initially move in random directions. In general, the drift field takes over and pushes the electrons in one direction and the holes in the other. It is necessary for the electrons and holes to reach the positive and negative electrodes, respectively, for the full ionization signal to appear on the amplifier. However, for events near the surface, it is apparently possible for some charge carriers to enter the incorrect electrode before the drift field can take over; hence they never reach the correct electrode and the full signal does not appear.

The electron hypothesis is greatly strengthened by data taken during exposure of a test device to a ^{14}C electron source, displayed in Figure 4. This device used an ionization contact similar to the one used on the BLIP detectors. Electron-induced events have suppressed ionization yield, pulling them down into the nuclear-recoil band. Why has this effect not been seen in previous low-background experiments? The sensitivity of the CDMS detectors to external electrons is an artifact of the ionization electrode used. Previous WIMP searches have used p-type Ge ionization detectors with coaxial contacts, the exposed outer contact being a 1 mm thick Li-drifted electrode. The electrode region is totally "dead", and hence such detectors never saw low-energy photons or electrons. Using such a contact in a phonon-mediated detector is not possible for technical reasons, though some kind of "totally dead"

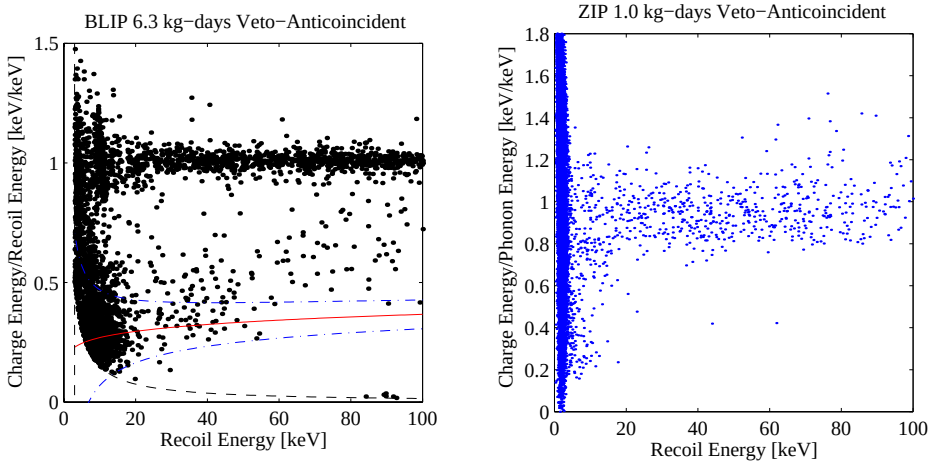

Figure 3. Veto-anticoincident ionization yield plots for BLIP and ZIP detectors in the spring 1998 run. For the BLIP data, the red (solid) line defines the center of the nuclear-recoil band; the blue dashed-dot lines are the edges. The hyperbolic black dashed line defines the ionization threshold. For the ZIP detector, the center of the nuclear-recoil band lies at approximately 0.5. There are two nuclear-recoil candidates above 25 keV; below 25 keV, noise causes the photon band to broaden and also reduces the surface event veto capability.

contact was considered initially.

Further evidence for the electron hypothesis comes from the ZIP detector, data from which are also shown in Figure 3. A cut removing events with fast phonon rise times has been made. This detector is made of silicon, so the nuclear-recoil band is expected to be at roughly 0.5 on the vertical axis. There are clearly only 2 nuclear-recoil candidate events. They are at high energy compared to what is seen in the BLIP data. However, without the phonon rise time cut, a population of low-ionization-yield events appears. As discussed earlier, a fast phonon rise time is indicative of an interaction very near the surface; this again suggests that low-energy electrons are the cause of the low-ionization-yield events.

The source of low-energy electrons is not clear. There are three obvious choices that are consistent with the data: a β contaminant in the bulk of the copper detector housings, a surface β contaminant on the inner surface of the detector housings, and a surface β contaminant on the detectors themselves.

The WIMP exclusion limits obtained with this set of detectors are displayed in Figure 5. The BLIP detector sensitivity is limited by the large number of electron events contaminating the nuclear-recoil band. Thanks to the fast phonon rise time cut, the ZIP detector recoil-energy band contains only two events. The ZIP WIMP sensitivity is instead limited by the target material, silicon. The WIMP interaction cross-section scales roughly as A^2 and the interaction rate scales as the number of target nuclei; hence, a germanium ZIP of the same volume and with the same observed recoil spectrum would yield a limit roughly 10 times better.

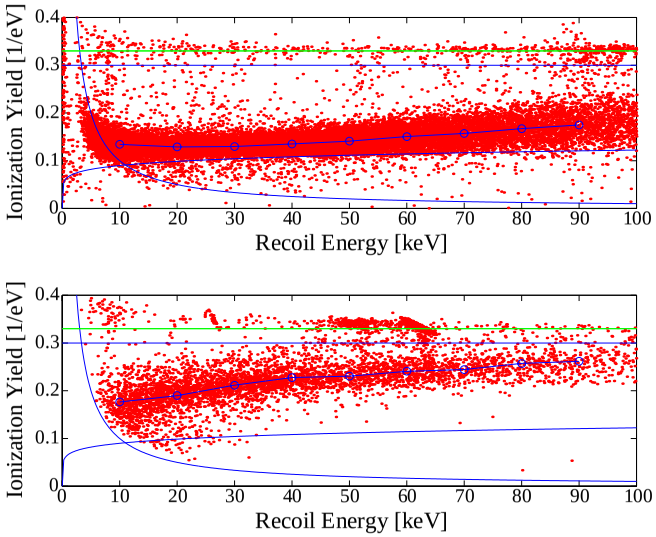

Figure 4. Data from exposure of two test devices to electrons from ^{14}C. The upper plot shows a device having an electrode similar to the one used in the BLIP detectors in the spring 1998 run. The lower plot shows a device using the new blocking electrode. For both plots, the vertical axis is ionization yield in charge pairs/eV, where 3 eV is the average recoil energy required to create an electron-hole pair. Photons lie at 1/3 and nuclear recoils at approximately 0.1, as indicated by the green (light) line and blue (dark) curve. The blue (dark) line curving down from the upper left indicates the ionization trigger threshold.

7. Reducing the Electron Background

To address the electron background problem, CDMS has pursued many avenues. As discussed above, fast phonon pulse shape discrimination works very well in identifying low-energy electrons. Germanium ZIPs are currently in testing and are expected to be deployed in fall 1999. Other techniques also promised gains and were being pursued before phonon pulse shape discrimination was demonstrated in spring 1998.

First among these complementary techniques was improvement of the dead layer. Essentially, the problem is that the ionization contacts do not block incorrect sign charges. CDMS tried a number of strategies for dealing with this and has arrived at a blocking contact design. Data from a test device using this contact are displayed in Figure 4. While the ionization collection for electrons does not fully recover to the photon value, the dead layer is clearly greatly improved. The center of the distribution lies well above the nuclear-recoil band and leakage into the nuclear-recoil band is less than 10%. CDMS has produced a set of 4 new Ge BLIP detectors using this blocking ionization contact.

Other techniques involved more traditional methods for combatting contamination in low-background experiments. Foremost was close-packing of the detectors. In the spring 1998 run, each detector had its own copper housing and thus was completely surrounded by copper. One possibility for the electron source was a β contaminant in or on the copper detector housing. To deal with this scenario, a detector housing was designed that placed the new detectors face to face and 3 mm apart with no intervening material. The new package accomplishes two things. First, due to the inner/outer

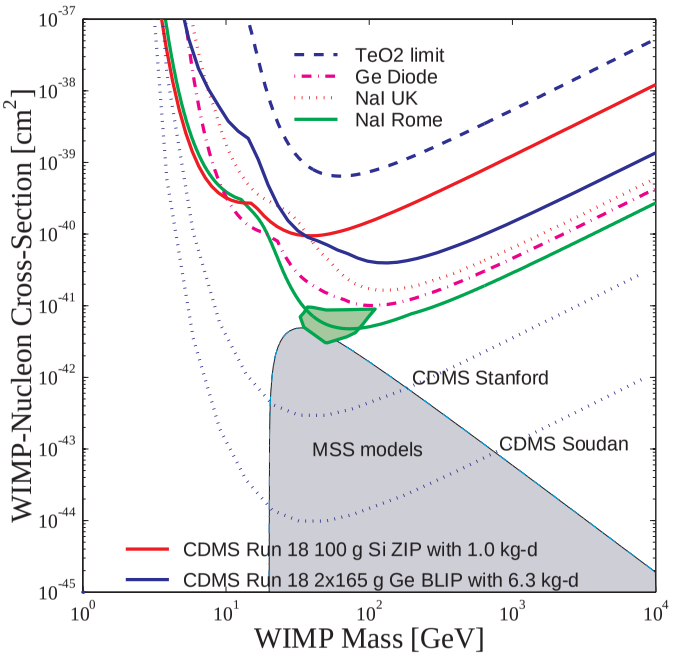

Figure 5. WIMP exclusion limits from CDMS spring 1998 run and for other experiments. The green heart-shaped region is the DAMA 3σ annual modulation detection. Also shown are expected final sensitivities of CDMS at SUF and at Soudan.

electrode design discussed earlier, the outer electrodes shadow the inner electrodes for a β source on the copper housing. This promises a factor of 5 reduction in electron rate on the inner electrode. Second, the geometry allows electrons that hit the inner electrodes to multiply scatter and produce signals in two adjacent detectors. Thus, even if the electron source were on the detectors themselves, such a geometry permits measurement and subtraction of the electron background, provided it is possible to infer the singles rate from the multiple-scatter rate using simulations.

Another improvement was to implement a cleanliness regimen that was far more stringent than used previously. This involved ensuring the detectors were never exposed except under class 100 clean room conditions and minimizing the time between production and installation in the cryostat. Last-minute etching and similar cleanliness precautions were undertaken for the detector housing also.

As a final precaution, roughly 90% of the exposed inner faces of the new copper detector housing was covered with 2 mm thick plates of detector-grade germanium, etched prior to installation. This thickness is sufficient to stop electrons up to 2 MeV. These plates were likely to be cleaner than the detectors and would thereby provide a second layer of defense against contamination in or on the copper housing. They would offer no help if the contamination were on the detectors themselves, but would allow discrimination between on-detector and copper contamination.

Finally, regarding the tritium problem: Of the two BLIP detectors in the spring 1998 run, BLIP2 displayed roughly 1/3 the tritium rate seen in BLIP1. The two detectors had been etched and the ionization contacts remade simultaneously, while their housings had been constructed and etched many months apart, so this strongly

pointed to the copper housing material. To test this hypothesis, the two detectors' housings were exchanged prior to the current run.

8. Results from the Current Run

A data run with the four new detectors (BLIPs 3 through 6) in their new housing and BLIPs 1 and 2 exchanged began in October, 1998. BLIPs 3 through 6 are stacked face-to-face vertically, BLIP3 on top, BLIP6 on bottom, in a single copper detector housing as described above. A total of 7 raw live-days of data were collected by mid-December, 1998. Assorted data-quality and veto-anticoincidence cuts reduce this to 4.5 live-days per detector, or 0.75 kg-days each. The total exposure is 3 kg-days. A preliminary analysis has been performed on these data.

Veto-anticoincident ionization yield plots for BLIPs 3 through 6 are displayed in Figure 6. Again, photons lie at roughly 1 on the vertical axis. A single-scatter cut has been applied because the likelihood of a WIMP multiply scattering is vanishingly small. A small correction must be made for the loss in efficiency for detection of accidental background-WIMP coincidences, however. The magenta lines define the nuclear-recoil acceptance band (the range of ionization yield as a function of recoil energy in which nuclear recoils fall). At high energy (where the trigger threshold does not result in a loss of efficiency), this band yields 90% acceptance. Two facts are obvious from these data. First, in all detectors, the inner electrode rate in the nuclear-recoil band is much lower than the outer electrode rate. Second, BLIP3 has a much higher rate, both overall and in the nuclear-recoil band. It should be noted that the tilted line at roughly 10 keV is a ^{68}Ga X-ray due to internal activation; the tilt arises because the denominator of the ionization yield parameter is correlated with recoil energy. Also, it is clear that the nuclear-recoil band definition is not optimal; the splaying of the band at low energy, and the resultant acceptance of events that are clearly photons, could be remedied with an acceptable loss of nuclear-recoil acceptance.

Recoil-energy spectra for the data in Figure 6 are displayed in Figure 7. In addition to the single-scatter cut, the outer electrodes of the detectors have been excluded, and the exposure has been correspondingly reduced to a total of 1.7 kg-days. As discussed earlier, it was expected that the outer electrodes would see more low-ionization-yield events from off-detector contamination. The total anticoincident event rate is roughly 1 kg^{-1} keV^{-1} day^{-1}, demonstrating a reduction of a factor of 2 in the total anticoincident event rate arising from cutting multiple scatters. The single-scatter nuclear-recoil rate is displayed in red; these are the inner electrode events falling in the nuclear-recoil acceptance bands defined in Figure 6. As noted above, the collection of events below 23 keV is actually dominated by photons due to the unsophisticated definition of the nuclear-recoil band. The spike at 32 keV corresponds to a single event in BLIP3.

Data from BLIPs 1 and 2 have also been collected. It is clear that the tritium has "moved": now BLIP2 displays a higher tritium rate than BLIP1, squarely isolating the tritium source to the copper detector housings.

Due to the preliminary nature of this analysis, an exclusion limit has not been derived from these data. However, it is instructive to take the event rates seen by other experiments and ask how many events would be seen with the CDMS 1.7 kg-days exposure. The two leading experiments are Heidelberg-Moscow (germanium ionization detectors) and DAMA (annual modulation search with NaI scintillator). HM sees 217 events in the recoil-energy region 27 to 60 keV with 251 kg-days [8], yielding 2.1 events

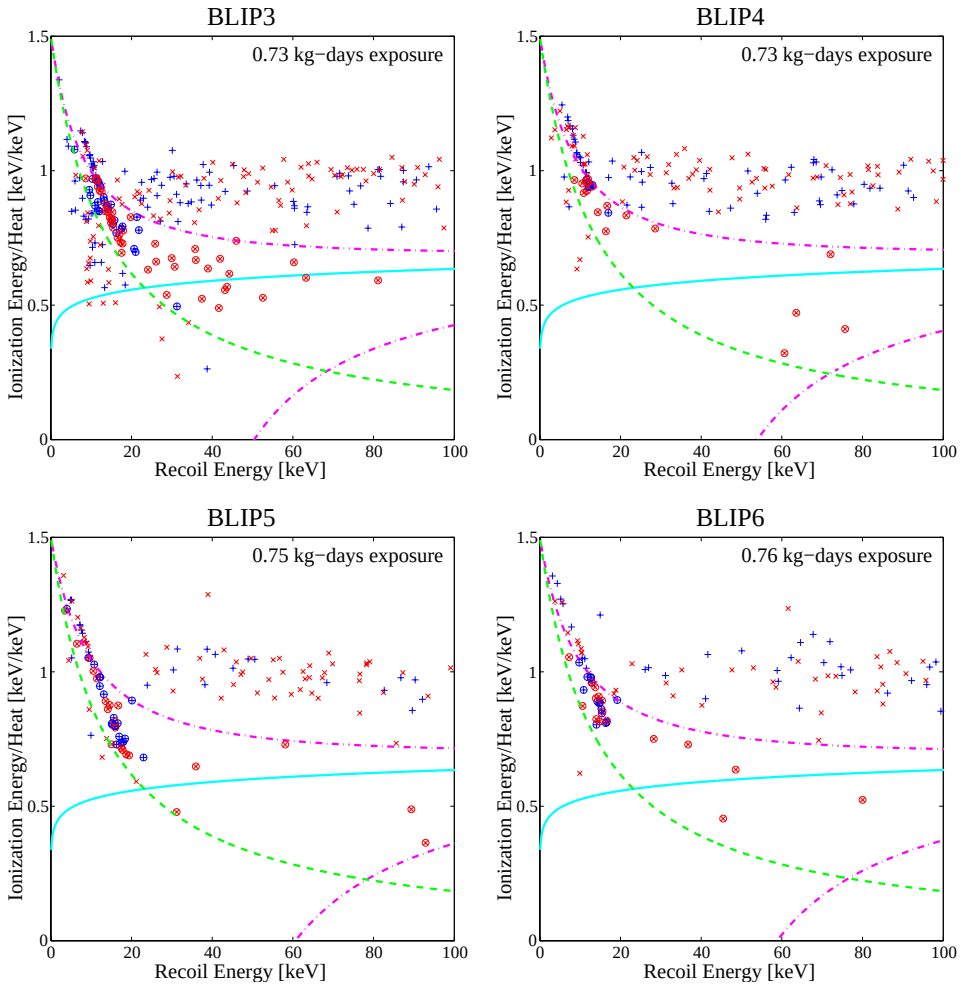

Figure 6. Veto-anticoincident ionization yield plots. The vertical axis is ionization/heat, where heat is the is the raw phonon signal, prior to subtraction of charge-drift generated phonons (*c.f.* Figure 2). Blue +'s are inner electrode events; red x's are outer electrode events. The cyan (solid light) line indicates the center of the nuclear-recoil band (it is raised to ~ 0.6 because the vertical axis is ionization/heat, not ionization/recoil). The magenta (dashed-dot) lines indicate a 90% acceptance band: -3σ to +1.28σ. The circled events (inner and outer) fall in the nuclear-recoil acceptance region. The green dashed line indicates the ionization threshold imposed during the analysis; only events above this line may be included (the efficiency is set to 0 below this line). Note the prominent 10.4 keV ^{68}Ga X-ray.

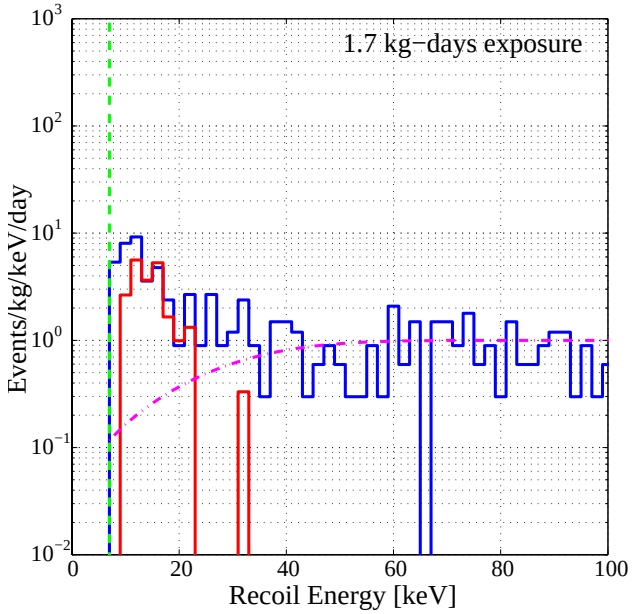

Figure 7. Veto-anticoincident recoil-energy spectra. The spectrum of all anticoincident single-scatter events is shown in blue (dark). The spectrum of single-scatter events in the nuclear-recoil band is shown in red (light). The magenta dashed-dot line indicates the nuclear-recoil efficiency as a function of energy, normalized to its high energy value. The loss of efficiency at low energy is due to the trigger threshold cutting into the nuclear-recoil acceptance region.

in that region with 1.7 kg-day exposure. DAMA's annual modulation amplitude [9] implies an unmodulated signal of 0.9 events/kg-day in the recoil-energy region 22 to 66 keV for iodine; scaling to Ge ($A_I^2/A_{Ge}^2 = 3.02$) and ignoring form factor effects (which would only enhance the Ge signal further) yields 0.5 events in this region. Both numbers should be scaled down by approximately 50% to take into account the reduction in nuclear-recoil efficiency below 40 keV. At present, CDMS sees 1 event above 25 keV. From these numbers, one can see that CDMS is becoming quite competitive.

Since the beginning of 1999, roughly 14 more live-days of data have been collected. This run will continue through September, 1999, so a factor of 10 to 20 increase in exposure will be achievable. In addition to increasing the exposure, the run has the goal of understanding the source of the residual electron background. One element of this is the high outer electrode rate on BLIPs 3 through 6. This could be due to an electron source on the detector housing or to depressed charge collection in the outer electrode in the vicinity of the top-bottom electrode break. Another aspect is to understand the high rate in BLIP3. It is unlikely that the detector housing is responsible, as all pieces went through the same production steps at the same time; one would expect BLIP6 to also have a high event rate. Two explanations remain. First, there is something outside the housing, above the detectors, that is interacting in the copper housing and producing electrons. The distribution of materials outside the housing is asymmetric, with material more likely to be contaminated or intrinsically radioactive lying above the detectors and hence more likely to affect BLIP3. Second,

BLIP3 may suffer worse surface contamination. BLIP3 was the prototype for BLIPs 4-6 and hence suffered more environmental exposure due to repeated processing and testing steps. The second option should result in an elevated rate in BLIP4 also; none is seen in the single-scatter data, but the multiple-scatter data have not been studied yet. Additional information will be provided by data taken at reduced ionization bias where the electron-induced event band may be more well-defined.

9. Conclusion

CDMS has demonstrated significant progress in reducing its electron backgrounds. This improvement has been due both to a new electrode technology that reduces the "dead layer" problem significantly and to detector mounting and production changes to reduce and shield contamination sources. CDMS is presently engaged in an extended run of the present set of detectors. A stack of 6 germanium ZIPs (1.5 kg total mass), combining surface event veto capability with improvements demonstrated in this run, will be deployed in fall 1999. Operation at the Soudan mine is expected to commence in summer 2000. Expected sensitivities for CDMS at SUF and at Soudan are shown in Figure 5.

Acknowledgments

We would like to thank John Emes, Dennis Seitz, Garth Smith, Eric Jones, and Evan Bierman for critical technical and engineering support during preparation of the detectors, hardware, and electronics used in this run, and Storn White for the design of a most bitchin' detector package. This work is supported by the Center for Particle Astrophysics, an NSF Science and Technology Center operated by the University of California, Berkeley, under Cooperative Agreement No. AST-91-20005, by the National Science Foundation under Grant No. PHY-9722414, and by the Department of Energy under contracts DE-AC03-76SF00098, DE-FG03-90ER40569, and DE-FG03-91ER40618.

References

[1] V. Trimble, *Ann. Rev. Astron. Astrophys.*, **25**, 425 (1987).
[2] K.A. Olive, these proceedings.
[3] P.J.E. Peebles, *Principles of Physical Cosmology*, Princeton University Press, 1993.
[4] G. Jungman, M. Kamionkowski, and K. Griest, *Phys. Rep.*, **267**, 195 (1996).
[5] J.D. Lewin and P. F. Smith, *Astropart. Phys.*, **6**, 87 (1996).
[6] H. Wang, *Phys. Rep.*, **302**, 263 (1998).
[7] J.D. Taylor, D.S. Akerib, P.D. Barnes, Jr., P.A. Luft, R.R. Ross, B.Sadoulet, R.V. Schafer, S. White and R.C. Wolgast, *Adv. Cryo. Eng.*, **41**, 1971 (1996).
[8] L. Baudis, J. Hellmig, G. Heusser, H.V. Klapdor–Kleingrothaus, S. Kolb, B. Majorovits, H. Paes, Y. Ramachers, H. Strecker, V. Alexeev, A. Bakalyarov, A. Balysh, S.T. Belyaev, V.I. Lebedev, S. Zhukov, *Phys. Rev. D*, **59**, 22001 (1999).
[9] R. Bernabei, P. Belli, F. Montecchia, W. Di Nicolantonio, G. Ignesti, A. Incicchitti, D. Prosperi, C.J. Dai, L.K. Ding, H.H. Kuang, J.M. Ma, ROM2F/98/34.